A SUBNANOWATT MICROBUBBLE PRESSURE SENSOR BASED ON ELECTROCHEMICAL IMPEDANCE TRANSDUCTION IN A FLEXIBLE ALL-PARYLENE PACKAGE

Christian A. Gutierrez and Ellis Meng
University of Southern California, Los Angeles, California, USA

ABSTRACT

We present the first all-Parylene microbubble pressure transducer (μBPT) harnessing the ability of a microbubble (μB) to respond instantaneously to external pressure variations. A μB is electrolytically generated and physically trapped within a Parylene microchamber such that pressure-induced bubble size variation is detected by electrochemical impedance (EI) measurement. Real-time hydrostatic pressure measurement (-11.8 Ω/psi, ±0.1 psi) of negative and positive pressures (-2 – 4psi) is demonstrated. The open-package device design leverages the ambient liquid environment obviating the need for hermetic packaging techniques. μBPTs are biocompatible, flexible, ultra-miniature (200 μm diameter, 10 μm thick), and can be operated at very low power (≤ nW) making them especially attractive for wet, *in vivo* pressure measurement.

INTRODUCTION

It is known that gas bubbles respond instantaneously to external pressure variations [1] at frequencies below resonance (55 kHz for a 50 μm bubble radius [2]), however few efforts have successfully exploited this phenomena for sensing. Polymer-based MEMS fabrication technology is leveraged here to enable a new class of transducer that can precisely produce, localize, and measure bubble response at micron scales, realizing a novel pressure sensor with unique capabilities (Figure 1).

State-of-the-art ultraminiature pressure sensing technologies generally occupy 400-500 μm diameter footprints. Our unique electrochemical-based pressure sensing technique does not utilize conventional diaphragm-based pressure transduction, enabling significant reductions in overall footprint, packaging complexity, and power consumption (Table 1). Parylene C is featured as both the flexible substrate and structural material enabling electrolytic bubble generation, localization, and transduction in a completely released and portable device compatible

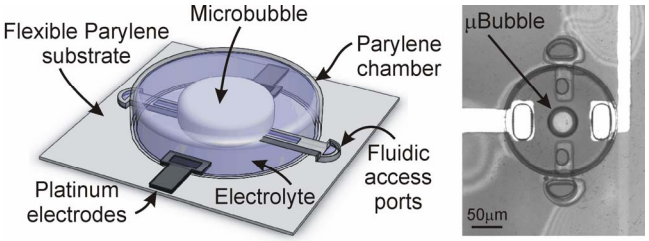

Figure 1: (Left) Model of pressure transducer. (Right) Optical micrograph of device (200μm diameter) with entrapped microbubble (50μm diameter).

Table 1: Comparison to other sensing modalities

Modality	Packaging	Power	Size
E-chemical	**Open**	**Low**	**<300 μm**
Piezoresistance	Hermetic	High	>500 μm
Capacitance	Hermetic	Low	>400 μm
Optical	Hermetic	low	>300 μm

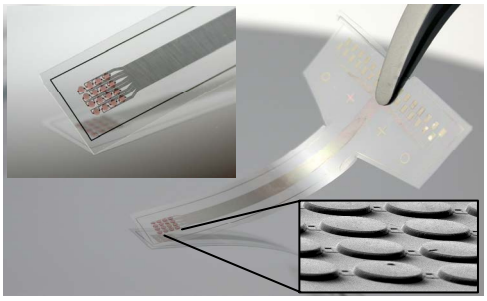

Figure 2: Completely released Parylene-based system with a 4×4 array of sensors (200 μm diameter). Sensor array is interfaced via an integrated flat flexible Parylene cable.

with various liquid environments (Figure 2). In particular, these features address the unmet need for robust *in vivo* pressure sensors. Our approach eliminates the need for hermetic packaging and the exclusive use of polymer materials reduces cost, adds mechanical flexibility, and streamlines integration for medical applications.

THEORY

Microbubble Dynamics

The fundamental dynamics of a suspended bubble fixed in an unbounded incompressible viscous liquid are governed by the Rayleigh-Plesset equation [3]:

$$r\ddot{r} + \frac{3}{2}\dot{r}^2 = \frac{1}{\rho}\left(p_g - p_\infty - \frac{2\sigma}{r} - \frac{4\mu}{r}\dot{r}\right) \qquad (1)$$

where r is the bubble radius (dot denotes time-derivative), p_g and p_∞ are the pressure in the gas at the bubble wall and ambient pressure far away from the bubble (infinite distance), σ is surface tension, μ is fluid viscosity, and ρ is fluid density.

Under the condition that the pressure oscillation frequency is much smaller than the bubble resonant frequency the following pressure-radius relationship is obtained:

$$p_\infty = p_i\left(\frac{r_0}{r}\right)^b - \frac{2\sigma}{r} \qquad (2)$$

where polytropic exponent $b \approx 1$. The pressure-radius response can therefore be estimated by Eq. 2 which

describes the balance of forces acting on the bubble. For a given number of gas molecules produced by electrolysis and a non-varying surface tension, bubble size is a direct and instantaneous measure of ambient pressure.

For bubble behavior over larger time scales, the effects of mass transfer at the bubble liquid interface become significant. The bubble will dissolve in the presence of an under-saturated liquid as a consequence of diffusion across the bubble-liquid interface. The bubble dissolution rate in an under-saturated solution was derived by Epstein and Plesset [1]:

$$\frac{dr}{dt} = \frac{k(c_s - c_\infty)}{\rho_\infty + 2\tau/3r}\left(\frac{1}{r} + \frac{1}{(\pi kt)^{1/2}}\right) \quad (3)$$

where k is the coefficient of diffusivity of the gas in the liquid; c_s and c_∞ are the saturation concentrations of gas in the liquid at the bubble surface and in the bulk, respectively; ρ_∞ the density of gas in the bubble with a gas-liquid interface of zero curvature; and τ is the modified surface tension. Henry's law establishes a connection between the partial pressure of gas acting on a liquid surface, p_g, and the equilibrium (or saturation) concentration of gas in the liquid:

$$c_s = ap_g \quad (4)$$

a is a constant characteristic of the particular gas–liquid combination and is a function of temperature. If the ambient pressure is fixed and equal to p_∞, then it is clear that unless the gas concentration c at the bubble surface satisfies Eq. 4, the bubble will not be in equilibrium, and will either grow or shrink when $c > c_s$ or $c < c_s$, respectively. Mass transfer driven bubble dissolution is a slow process; typical values for bubbles of radius ~100 μm are estimated to be on the order of ~0.1 μm/sec [3].

Electrochemically-based Transduction

The underlying principle of electrochemically-based transduction is the measurement of solution impedance. By applying a small alternating current across a pair of electrodes (at a sufficiently high frequency, typically >1 kHz), the solution resistance can be measured. The electrical response of this system has been well characterized in literature [4]. Electrochemical measurements are possible at nanowatt power levels, making this approach attractive for wireless and implantable applications. The solution resistance is a function of ionic concentration, distance between the electrodes, and cross-sectional area of electrolyte between the electrodes. A trapped μB acts as an insulating sphere in the conductive incompressible electrolyte between the electrodes. Therefore, the monitoring of μB size variations by measuring electrolyte impedance (resistance) correlates to external pressure variations (Figure 3). Previously, pressure measurements within a microfluidic channel were demonstrated using μBs and electrochemical impedance transduction [5], however this approach utilized rigid substrate materials and was limited to measurement of intra-channel pressure.

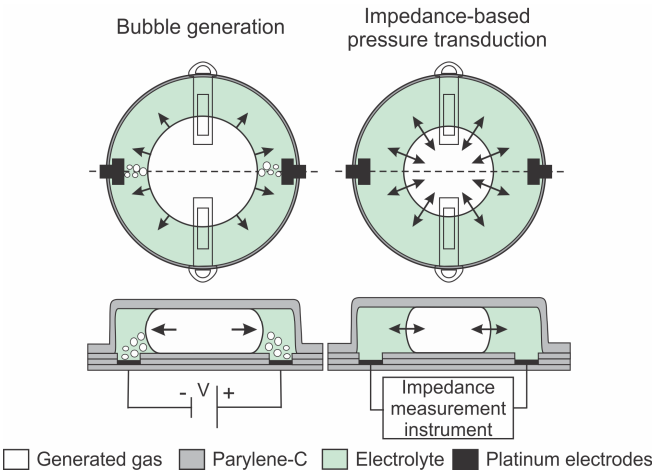

Figure 3: (Left) Electrolytic μB generation and localization within the Parylene microchamber. (Right) Bubble size instantaneously responds to external pressure and is tracked by electrochemical impedance measurement. Top row = top views, bottom row = cross-sections.

METHODS

Materials and Fabrication

The transducer features all-Parylene construction with thin film platinum electrodes and traces. No further materials are utilized nor any hermetic sealing or encapsulation techniques required. The open-package design enables a "wet" sensor that is open to, and filled by, the surrounding aqueous liquid (via fluidic access ports) which becomes the electrolyte in the sensor (Figure 1). Isolation of the sensor from the environment is therefore not necessary and the added costs and complexities of hermetic packaging are avoided.

Fabrication techniques were previously reported [6]. Briefly, platinum electrodes (2000 Å) were deposited and patterned on a Parylene coated (10 μm thick) soda lime wafer followed by a 1 μm thick Parylene insulation layer. A 2 μm sacrificial photoresist layer then formed the fluidic access ports followed by a second Parylene deposition step (2 μm thick). A 10-12 μm sacrificial photoresist layer was then spun-on and patterned to establish the chamber height and diameter (200 μm). The chamber structure was enclosed by a final 4.2 μm Parylene layer, followed by opening of access port vias by oxygen plasma (Figure 4).

Following removal of sacrificial photoresist by immersion in acetone and isopropyl alcohol, devices were simultaneously filled at the wafer-level by passive soaking in a bath of the desired electrolyte solution. The chamber design allows the ionic conductive path to be constrained within a known geometry and minimizes the potential for cross talk between adjacent sensors.

Experimental Setup

The devices were filled with 1x phosphate buffered saline (PBS) as the electrolyte. A microbubble was electrolytically generated within the chamber by applying a DC current pulse (typically 1 μA, 5 s).

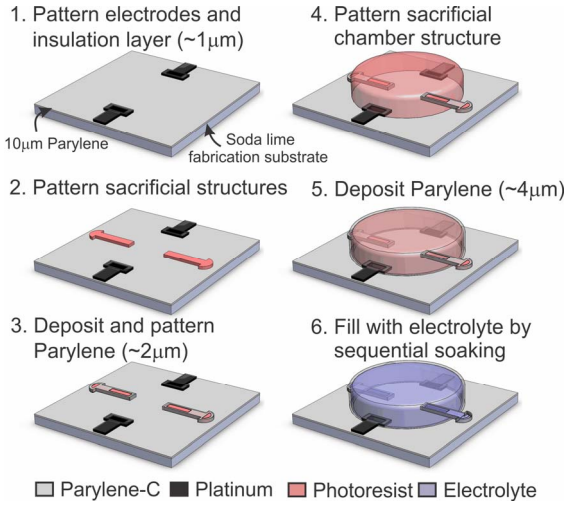

Figure 4: Fabrication process flow for a single transducer.

Device impedance was monitored using a LabVIEW-interfaced precision LCR meter (1 V_{pp}, 5 kHz) (Agilent E4980A). A calibrated pressure source metered external hydrostatic pressure to the μBPTs housed in a test jig.

RESULTS AND DISCUSSION

Hydrostatic Pressure Measurement

Hydrostatic pressure oscillations were applied between -2 and 4 psi (-100-200 mmHg). Impedance measurements tracked applied pressure closely (inversely) and exhibited excellent resolution over this range (Figure 5). Measurements were obtained within 100 seconds of bubble formation; minimal change in bubble volume occurred over this time. Measurement of discrete pressure steps was also possible and demonstrated previously [7]. A calibrated sensor response of -11.88 Ω/psi was obtained by a best fit linearization and clearly demonstrated pressure tracking capability (Figure 6). Pressure measurement resolution was estimated to be ±0.1 psi (689.4 Pa) as determined by the minimum detectable pressure variation. It was also possible to detect pressure variations at excitation powers less than 1 nW (100 mVpp, 10 nA) with a signal-to-noise ratio >20 to achieve sub-nanowatt device operation (Figure 7). The bubble generation phase does require somewhat higher power levels but these are typically in the microwatt range and only a few seconds in duration. Wireless μB generation via inductive coupling (2 MHz, Class D) was achieved for distances greater than 5 cm and <5 μW at the secondary (Figure 8). However, complete wireless operation still requires implementation of wireless impedance measurement, which has been demonstrated by others [8].

Alternative device configurations are also possible; for example, devices may utilize a trapped electrolyte that differs in composition from the surrounding medium. This can be realized through integration of liquid entrapment structures, such as a Parylene-based stiction valve [9]. This capability, combined with the small size, polymer construction and low power operation makes this approach attractive for wireless pressure monitoring.

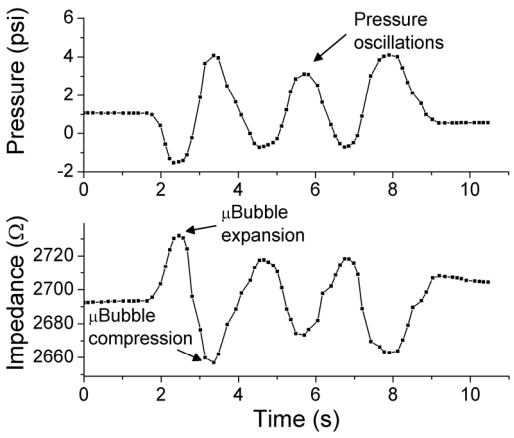

Figure 5: (Top) Profile of applied hydrostatic pressure from calibrated pressure source. (Bottom) Measured μBPT impedance response (1x PBS) to applied pressure profile.

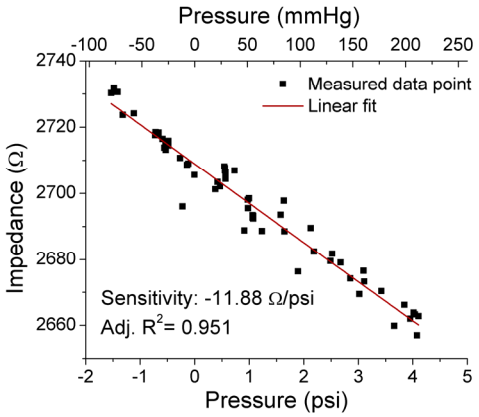

Figure 6: Impedance data from figure 5 plotted against pressure. Response is linear and yields excellent sensitivity.

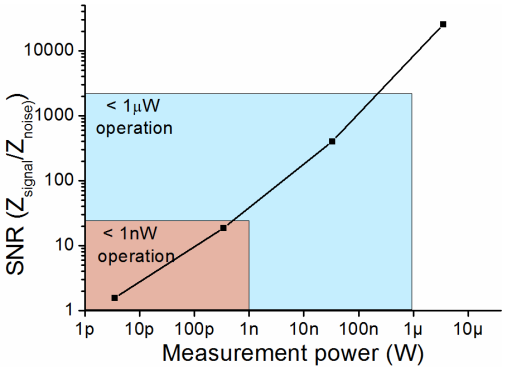

Figure 7: Subnanowatt EI measurement possible with >20 SNR making technique attractive for wireless applications.

Measurement Application

Operation was demonstrated in the real-time tracking of internal pressure in an electrolysis pump utilized in a MEMS drug delivery system [10]. The μBPT was placed in contact with fluid in the pump chamber. Pump on/off states were clearly detected and calibrated pressure measurements agree well with previously reported data measured with a conventional silicon pressure transducer (Figure 9).

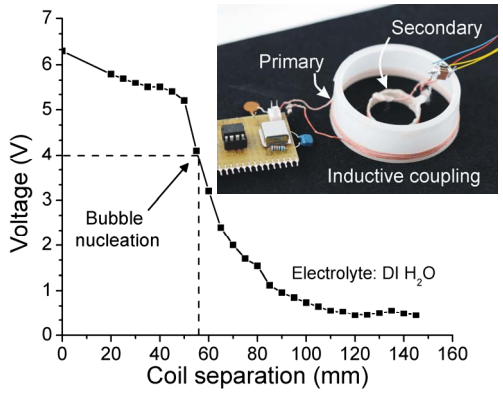

Figure 8: μBs were successfully generated via inductive coupling at distances greater than 5 cm and currents <1 μA using DI water as the electrolyte. Bubble nucleation was observed at power levels typically <5 μW.

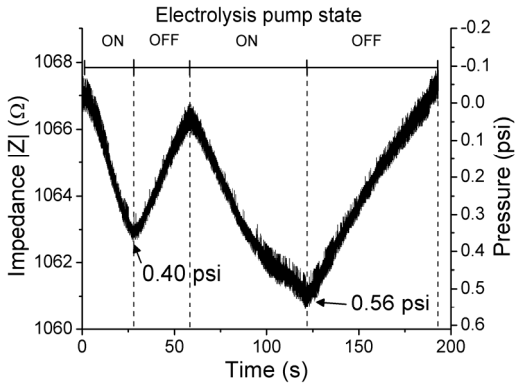

Figure 9: Impedance response to electrolysis pump activation/deactivation cycles (5 mA pump current). Calibrated measurement of pressure (-10.7 Ω/psi) is shown at two points.

Static Bubble Approximation

Once the bubble is formed, the slow diffusion-limited dissolution process maintains an approximately constant bubble size for a period of time (~20 min), and is dependent on the kinetics and solubility of the gas/liquid interface. Generally, smaller bubbles will have higher surface tension and therefore higher internal pressures which serves to speed up the dissolution according to Eq. 1. In our design, the platinum electrodes are located at the periphery of the chamber, limiting contact between the recombining gas and the electrodes, thereby minimizing any catalytic effect. In addition, the bubble is compressed due to the fixed chamber height and is forced to expand only in lateral directions, thus the top and bottom surfaces of the bubble, which are in contact with the chambers top and bottom surfaces, do not contribute significantly to the mass transport process.

These factors, taken together, give rise to longer bubble lifetimes allowing their use as quasi-constant pressure sensors over short to medium time scales (~15-20 min). Other electrolyte-gas combinations can be utilized, such as ethylene glycol or alcohols, which may provide insoluble conditions for entrapped gases for applications requiring long term constant-volume μB transduction capability.

CONCLUSION

We have designed, fabricated and tested a Parylene-based pressure transducer utilizing a unique liquid-impedance transduction technique. Microbubbles were harnessed as transducers to electrochemically monitor pressure. The sensor operates in communication with the surrounding liquid environment (either DI water or PBS), thereby eliminating the need for hermetic packaging and shows promise for low-power wireless applications.

ACKNOWLEDGEMENTS

This work was funded in part by the Engineering Research Centers Program of the NSF under Award Number EEC-0310723, an NSF CAREER Award (ECS-0547544), and the Bill and Melinda Gates Foundation (CG).The authors would like to thank Dr. Donghai Zhu, Mr. Connor McCarty, Ms. Roya Sheybani and the members of the USC Biomedical Microsystems Laboratory for their assistance.

REFERENCES

[1] P. S. Epstein and M. S. Plesset, "On the stability of gas bubbles in liquid-gas solutions," *J. Chem. Phys.*, vol. 18, pp. 1505-1509, 1950.

[2] B. Ran and J. Katz, "The response of microscopic bubbles to sudden changes in ambient pressure," *J. Fluid Mech.*, vol. 224, pp. 91-115, 1991.

[3] M. S. Plesset and A. Prosperetti, "Bubble dynamics and cavitation," *Ann. Rev. Fluid Mech.*, vol. 9, pp. 145-185, 1977.

[4] J. E. B. Randles, "Kinetics of rapid electrode reactions," presented at Discussions of the Faraday Society, 1947.

[5] D. A. Ateya, A. A. Shah, and S. Z. Hua, "Impedance-based response of an electrolytic gas bubble to pressure in microfluidic channels," *Sensors and Actuators A*, vol. 122, pp. 235-241, 2005.

[6] C. A. Gutierrez, C. McCarty, B. Kim, M. Pahwa, and E. Meng, "An Implantable All-Parylene Liquid-Impedance based MEMS Force Sensor," in *IEEE MEMS*. Hong Kong, China, 2010, pp. 600-603.

[7] C. A. Gutierrez and E. Meng, "Subnanowatt Microbubble Pressure Transducer," in *Hilton Head: Solid-State Sensors, Actuators and Microsystems Workshop*. Hilton Head, SC, 2010, pp. 57-60.

[8] X. Zhang, J. Yan, B. Vermeire, F. Shadman, and J. Chae, "Passive Wireless Monitoring of Wafer Cleanliness During Rinsing of Semiconductor Wafers," *IEEE Sensors*, vol. 10, pp. 1048, 2010.

[9] C. A. Gutierrez and E. Meng, "Improved Self-Sealing Liquid Encapsulation in Parylene Structures by Integrated Stackable Annular-Plate Stiction Valve," in *IEEE MEMS*. Hong Kong, China, 2010, pp. 524-527.

[10] P.-Y. Li, R. Sheybani, C. A. Gutierrez, J. T. W. Kuo, and E. Meng, "A Parylene Bellows Electrochemical Actuator," *J. Microelectromech. Syst.*, vol. 19, pp. 215-228, 2010.